Simulation of the COVID-19 pandemic on the social network of Slovenia: effective strategies of the virus containment

Žiga Zaplotnik, Aleksandar Gavrič, Aleks Jakulin

April 3, 2020

Abstract

The ongoing COVID-19 pandemic has revealed a gap in our ability to forecast the evolution of the epidemic. While the widely used compartment models [1, 2] are a reliable tool to analyse the basic dynamic properties of the virus transmission [3], they struggle to represent the impact of the intervention measures on the virus spread in advance, especially in the declining stage of the epidemic, when the infected population is low and the assumption of homogeneous mixing becomes invalid [4]. Here, we have constructed a social network of more than 2 million nodes, each representing an inhabitant of Slovenia. The nodes are organised and interconnected according to the real household and elderly care center distribution, while their connections outside these clusters are semi-randomly distributed. The virus spread model is coupled to the disease progression model. Here, we compare the efficiency of strategies for the coronavirus impact mitigation and containment such as central quarantine and contact tracing. We show that people who infect many others, so called superspreaders, become increasingly important also in the declining stage of the epidemic. The ensemble approach with perturbed disease spread parameters and clinical parameters is used to quantify the ensemble spread, a proxy for forecast uncertainty. Such network models also allow to assimilate real-time data of the network properties, such as connectivity based on the mobile traces or mobility data. It also allows to assimilate the data about positively tested and patients such as age, sex and comorbidities. The approach should mimic an already established data assimilation approach in numerical weather prediction [5, 6] to make us more prepared for the next big pandemic.

1 Introduction

There are several ways to simulate the pandemic dynamics. The most common approach is to solve a system of differential equations given some predefined parameters. These epidemic models are widely known as susceptible (S), immune (I), recovered (R), i.e. SIR models [1, 2]. Another variation of SIR models is SEIR model, which accounts also for the exposed (E) - infected subjects which are not yet infectious themselves. SEIR models are combined with complex transfer or activation functions which are used to smoothly model social factors affecting virus spread, disease progression and to account for the probability distributions of their length. A major setback of the deterministic epidemic models is that they are only valid for sufficiently large populations [7].

In this study, we perform computationally more expensive node-based approach to simulate the virus spread. We simulate the spread over a realistic social network of more than 2 million nodes with a total of up to 15 million connections, representing the population of Slovenia and the connections of their inhabitants. A hard-to-overcome limitation of the SIR model and its variants is that the information is homogeneously spread. In reality, there are some who spread the information or virus more - so called superspreaders. Another advantage of such approach is that it allows to realistically simulate the quarantine orders of the decision bodies. Furthermore, it allows to simulate strategies for the disease containment and optimal case testing strategies. [8, 9] Section 2 describes the model and its parameters. Section 3 demonstrates four different deterministic scenarios of the pandemic dynamics. Section 4 presents the results and the most

k persons in household	number of k-person households
1	269898
2	209573
3	152959
4	122195
5	43327
6	17398
7	6073
8	3195
25	100 care centers with 8 groups each

Table 1: Households distribution in Slovenia.

likely outcome of the epidemics based on the ensemble computations which include the uncertainty of the input parameters. Section 5 discusses the potential strategies for the control of the COVID-19 pandemics. Discussion, conlusions and further outlook are given in Section 6.

2 Methodology

2.1 Social network model

The social network of the inhabitants of Slovenia is constructed based on the recent data of Statistical Office of Republic of Slovenia [10]. A total of $N = 2045795$ nodes is used in the social network. The number of k-person households is given in Table 1. There are approximately 100 elderly care centers in Slovenia with a total of approximately 20000 residents. Each elderly care center is assumed to include 8 distinct groups of 25 people.

Average household/care group has 2.5 people in Slovenia so the average number of contacts per person within household is 1.5.

Connectivity distribution in normal conditions follows power law distribution with fat tails [11], which are associated with superspreader events in pandemic dynamics. However, since all public events are canceled, those fat tails are cut off [12] and the topology of the social network changes drastically. In quarantine conditions, a reasonable assumption is to model the connectivity, i.e. the number of contacts per person using the gamma probability distribution, which is essentially an exponential distribution

$$p(x; k, \theta) = \frac{1}{\Gamma(k)\theta^k} x^{k-1} e^{-\frac{x}{\theta}}. \tag{1}$$

In this study, we used $k = 0.3$ and $\theta = 22.5$ for the initial setup, which gives an average number of 13.5 outer contacts per person per day (Figure 1). Together with 1.5 family contact per day, the total number of contacts per person per day is 15. Here, we assume that the average contact number is the same for each age group, despite studies showing seniors have reduced number of contacts already in normal conditions [13]. Another study shows that Italians have on average almost 20 contacts per day, Germans around 13.5, so 15 contacts per day is a reasonable guess for Slovenia [14].

Technically, we connect the graph in the following way

1. numbers of contacts for each node are randomly drawn from Gamma distribution (1). If node i has $x_i = 0.33$ contacts per day, it means that it will have 0 contacts 2/3 of the time and 1 contact 1/3 of the time of the simulation

2. for each node i we randomly assign the connections to x_i other nodes, where x_i is the number of contacts of node i. However, the assignments do not have equal probability. Node j which has x_j contacts is picked as a neighbour with probability $x_j N(x_j)/T$, where $N(x_j)$ is the number of nodes with x_j contacts and T is the total number of contacts in the network,

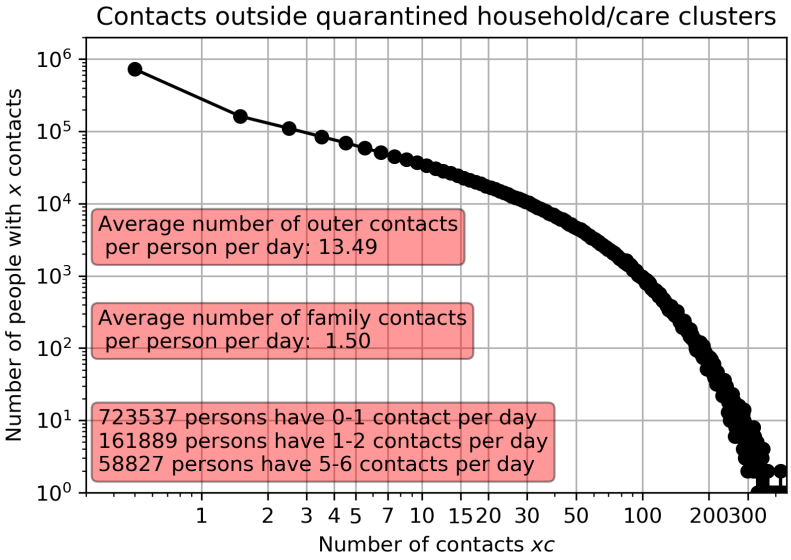

Figure 1: Number distribution by the number of contacts in social network.

two times the number of connections. Sampling over Gamma distribution (1) gives us a distribution of $N(x) = p(x)N$. When picking the neighbours, we actually sample the same Gamma distribution times x, i.e.

$$p_n(x) = p(x; k, \theta)x = \frac{1}{\Gamma(k)\theta^k} x^k e^{-\frac{x}{\theta}} \propto p(x; k+1, \theta) \tag{2}$$

3. The shape of the social network is changing at every time step of the simulation to account for people's mobility. (a) The number of contacts of node i is fixed (randomly jumps between $\lfloor x_i \rfloor$ and $\lceil x_i \rceil$ based on the value of x_i). For example, if a node has 0.33 contacts per day, 1 contact is picked with probability 1/3 and 0 contacts with probability 2/3. (b) The social network is rewired at every time step to account for superspreaders mobility. Note that rewiring might not be a good choice for those with low number of contacts.

2.2 Virus spread parameters

Reproduction number R_0 A basic reproduction number, R_0, only provides the info on the average dynamics of transmission, however it is crucial to understand what settings drive the virus spread. Different methodologies produced different results, however the majority of reported numbers is within 2 and 3. Here, we use median reported R_0 from a number of studies, as well as its median confidence intervals, i.e. $R_0 = 2.68$, with 95% confidence interval $[2, 3.9]$. This approach is surely not the optimal one, since we are trading accuracy for precision. The published R_0 values as well as our deduced R_0 distribution is shown in Figure 2. The optimal log-normal distribution should match the following conditions:

- $\mathrm{CDF}(R_0^L; \mu, \sigma, \Delta x) = 0.05$,
- $\mathrm{CDF}(R_0^H; \mu, \sigma, \Delta x) = 0.95$,
- $\mathrm{median}(\mathrm{CDF}) = \mathrm{R}_0$,

where CDF stands for log-normal cumulative distribution function, i.e.

$$\mathrm{CDF}(x; \mu, \sigma, \Delta x) = \frac{1}{2} + \frac{1}{2}\mathrm{erf}\left[\frac{\ln(x - \Delta x) - \mu}{\sqrt{2}\sigma}\right] \tag{3}$$

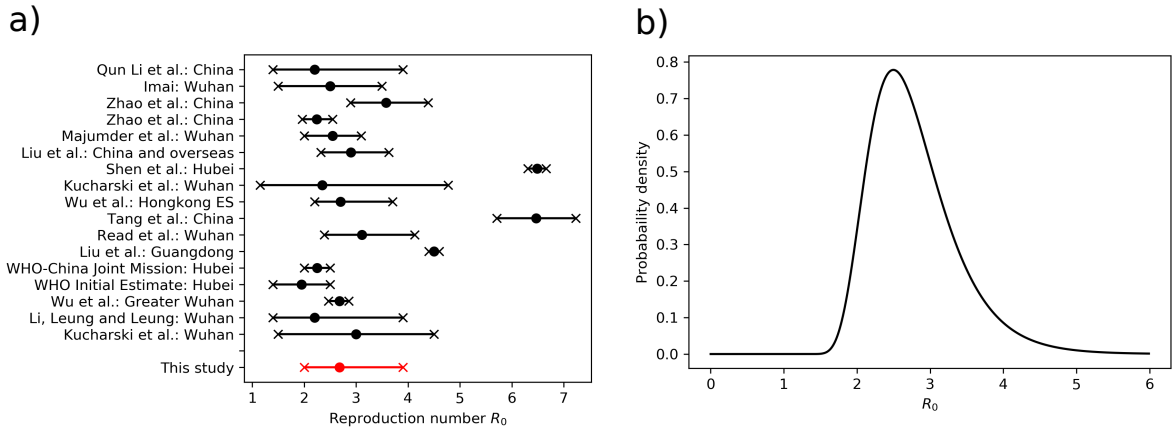

Figure 2: a) Basic reproduction number R_0, reported in number of studies, which can be found in Wu et al. [15], Kucharski et al. [16], Li et al. [9], Liu et al. [17] and references therein. b) Log-normal probability density function of the basic reproduction number, used for ensemble simulations.

and median being $\exp(\mu)$. Then, we define a quadratic cost function, which includes all the above criteria, and by minimizing it, we obtain the optimal parameters for log-normal distribution: $\Delta x = 0.36, \sigma = 1.14, \exp \mu = 1.54$.

Attack rate In general, the basic reproduction number, R_0 can be decomposed into the secondary attack rate times the number of contacts. The secondary attack rate (SAR) is defined as the probability that an infection occurs among susceptible people within a specific group (i.e. household or other close contacts). The measure can provide an indication of how social interactions relate to transmission risk. We can further decompose the R_0 into the household risk of infection and outer risk of infection (following [18])

$$R_0 = SAR_h N_h + SAR_c N_c, \tag{4}$$

where SAR_h and SAR_c are secondary attack rates within household and outside household (outer contacts) and N_h and N_c are the numbers of risk contacts made. The study of Liu et al. [18] suggest SAR_h value of 35% (95% CI 27-44%).

SAR_h is almost normally distributed with mean 35% and $2\sigma \approx 8.5$. The distribution of R_0 is given in the previous paragraph. It holds: $SAR_c = (R_0 - SAR_h * N_h)/N_c$. This gives a transmission efficiency of $SAR_c = 0.16$. Figure 3 shows probability distributions of secondary attack rates as used in the ensemble of simulations.

Given the infectious period of $T_{inf} \approx 10$ days (incubation period $T_{inc} \approx 5$ days minus 2 days + another week, check subsection 2.3), we can assume that the daily risk of getting infected from a certain household member is $SAR_{h,daily}$ where $1 - (1 - SAR_{h,daily})^{10} = SAR_h$ and

$$SAR_{h,daily} = 1 - \exp\left(\frac{1 - SAR_h}{T_{inf}}\right) \tag{5}$$

being equal 4.2% (3.1-5.6%). Similarly, we compute $SAR_{c,daily} = 1.7\%$.

Some studies [e.g. 19] have concentrated only on the symptomatic secondary attack rates and have shown relatively smaller numbers: 0.45% (CI=0.12%-1.6%) among all close contacts and 10.5% (CI=0.12%-1.6%) among household members. However, these numbers cannot reproduce the reported R_0 between 2 and 3.9 with realistic number of contacts. Another study shows similar attack rates we use in this study [20].

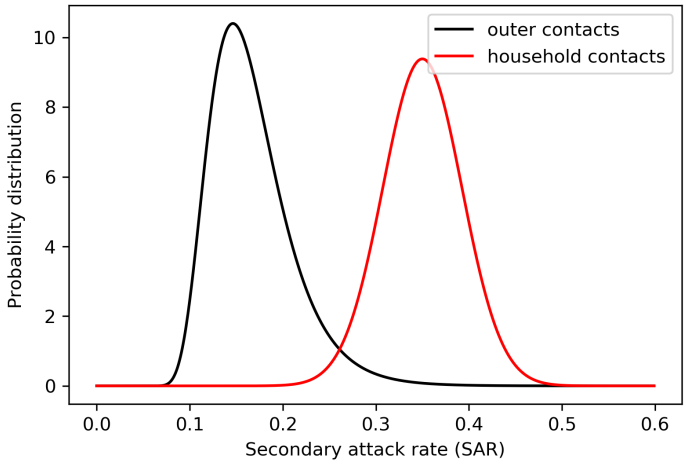

Figure 3: Probability distribution of secondary attack rates for household contacts and outer contacts.

2.3 Disease and hospitalization parameters

A simplified sketch of the simulation is shown in Figure 4. Note that for every node, that illness evolves differently based on the probability distribution described below. Note that for every member of the ensemble, the parameters of the distributions are perturbed according to known statistical values.

Case fatality ratio The baseline case fatality ratio (CFR), fatality ratio among all positively tested, is assumed 1.38% (CI 1.23-1.53%) [21, 22]. Dividing deaths-to-date by cases-to-date leads to a biased estimate of CFR, called naive CFR (nCFR) as the delays from confirmation of a case to death is not accounted for, as well as due to under-reporting of cases. The reported numbers agree with recently published study for symptomatic case fatality ratio in China [23].

Infection fatality and hospitalisation ratios Infection fatality ratio (IFR) estimates are based on the study from Verity et al. [21] and are taken to be 0.9% with 95% confidence interval 0.4% to 1.4% (95% CI is 2σ for normal distribution). These estimates are consistent with IFR on Princess Diamond Cruise ship and were used also in Ferguson's Imperical College report [24]. However, the countries vastly vary in demography. The study was performed for China with median age of 37.4 years. Slovenia has a median age of 44.5 years. The study also found an increasing infection fatality profile in age (Table2). These profile is used to determine the effective infection fatality rate for Slovenia. Performing a weighted average, we use the total IFR of 1.16% (CI 0.63-2.22%). Analogously, we compute the average hospitalisation rate of 6.37% (95% CI 3.8-13%). Using the minimization procedures, we obtain parameters of log-normal distribution which best fits both values and their 95% confidence interval (Figure 5).

Incubation period - infection to illness onset Mean incubation period is taken to be 5.0 days (95% CI 4.2-6.0), while the 95th percentile of the distribution was 10.6 days (95% CI 8.5-14.1) and 99th percentile 15.4 days (99% CI 11.7-22.5) [26]. Similar numbers were reported in an earlier study which included less patients [9, 27]. Log-normal distribution is used among for incubation period among nodes. However, the parameters of the lognormal distribution remain fixed due to numerical instability of their computation. Thus, all ensemble members have the same log-normal distribution of incubation period. Incubation period distribution and other outcome parameters are shown in Figure 6.

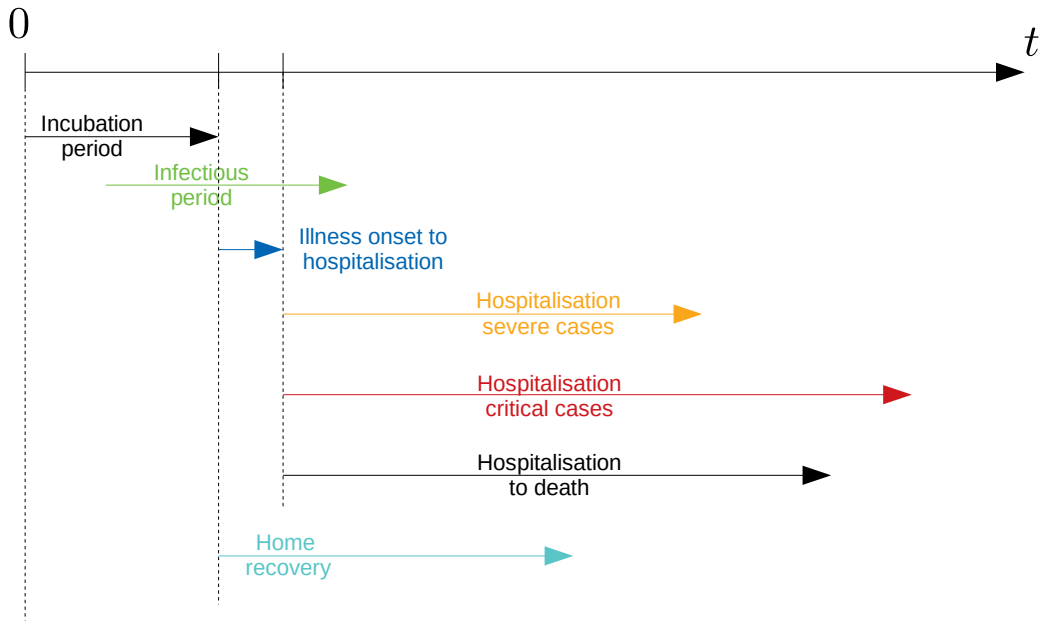

Figure 4: Simplified sketch of illness evolution.

Age group	IFR (95% CI)	IHR (95% CI)	Ratio of total population in SLO
0 to 9	0.0016% (0.000185,0.0249)	0% (0,0)	0.102
10 to 19	0.007% (0.0015,0.050)	0.04% (0.02, 0.08)	0.093
20 to 29	0.031% (0.014,0.092)	1.1% (0.62, 2.1)	0.102
30 to 39	0.084% (0.041,0.185)	3.4% (2.1, 7.0)	0.140
40 to 49	0.16% (0.076,0.32)	4.3% (2.5, 8.7)	0.146
50 to 59	0.60% (0.34,1.3)	8.2% (4.9, 16.7)	0.145
60 to 69	1.9% (1.1,3.9)	11.8% (7.0, 24.0)	0.135
70 to 79	4.3% (2.5,8.4)	16.6% (9.9, 33.8)	0.083
80+	7.8% (3.8,13.3)	18.4% (11.0, 37.6)	0.054

Table 2: Estimates of the proportion of all infections that would be hospitalised (IHR) or fatal (IFR) by age group. Disease data from Verity et al. [21]. Population data from PopulationPyramid.net [25].

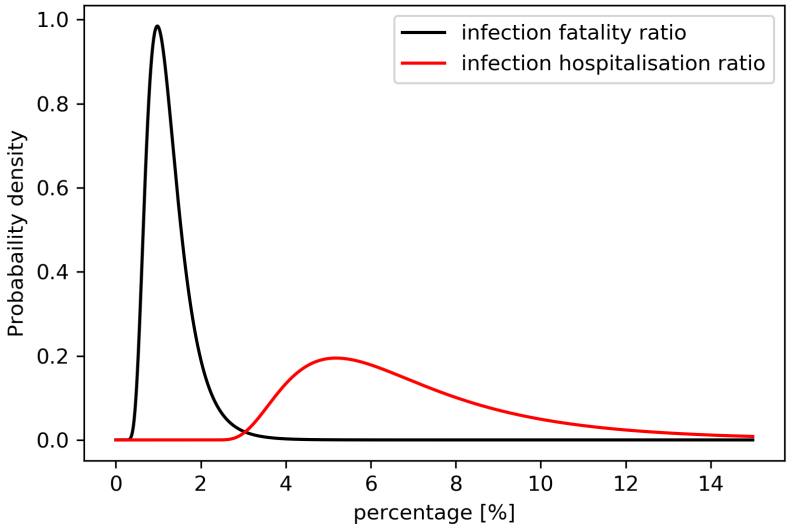

Figure 5: Infection fatality ratio distribution and infection hospitalisation ratio distribution for ensemble simulations.

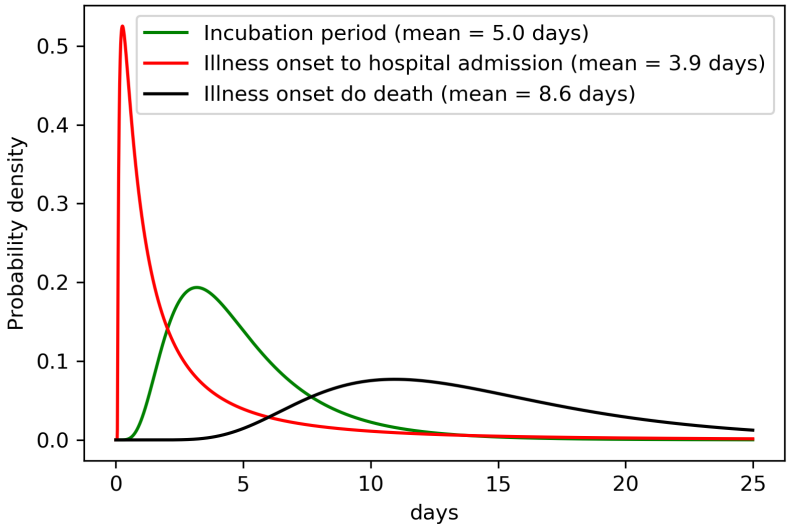

Figure 6: Incubation period, illness onset to hospitalisation and illness onset to death distribution among COVID-19 patients.

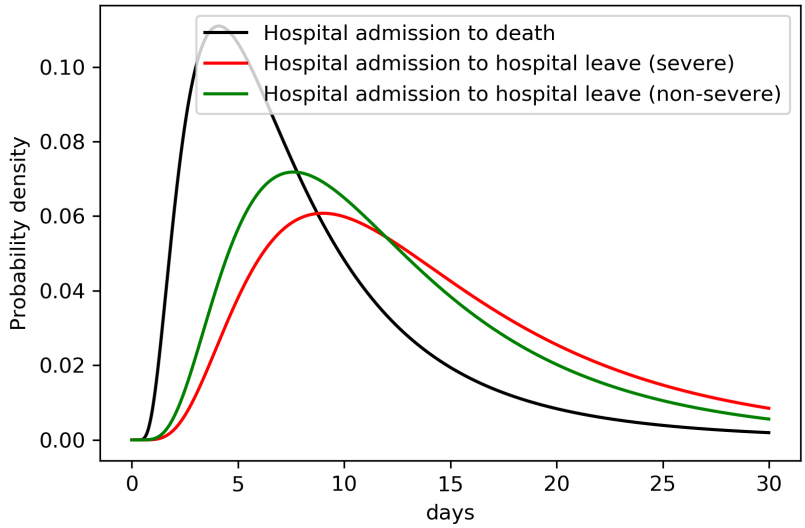

Figure 7: Mean distribution of hospital admission to death, hospital admission to hospital leave for severe and for non-severe illness.

Infectious period The infectious period starts $T_{start} = 2$ days before the end of incubation and likely ends around day $T_{end} = 5$ from symptoms onset [28], i.e. $T_{inc} - T_{start} + T_{end} \approx 10$ days, where average incubation period lasts 5 days. Note that none of the interval boundaries are known exactly, however several cases are known where infected transferred the virus before developing symptoms. Thus, we randomly perturb $T_{start} = \mathcal{N}(3, 0.5)$. The final boundary of the interval is more tricky, as it is dependent on the length the infectious person interacts with surroundings. Currently, we do not have a central quarantine for positively tested cases, however the infectious with symptoms are likely to more strictly isolate themselves, thus $T_{end} = \mathcal{N}(2.5, 0.5)$. Thus, whole families or elderly care centers get infected. The infectious period fall in line with study of Bi et al. [20], Figure S2.

Illness onset to hospital admission We take mean numbers from the study of Linton et al. [26] and its distribution: mean is 3.9 days, median 1.5 days, 5% percentile at 0.2 days and 95% percentile at 14 days. Since we now understand the severity of the illness, only the distribution of data for living patients is accounted for. In China, those who died waited longer to visit the doctor.

Illness onset to death Mean 14.5 days, median 13.2 days, 5th percentile 6.5, 95th percentile 26.8 [26]. Similar numbers were reported by Russell et al. [22].

Hospital admission to death Mean 8.6 days, median 6.7 days, 5th percentile 2.2, 95th percentile 20.5, 99th percentile 32.6 days [26]. Shown in Figure 7

Hospital admission to hospital leave Hospital admission to recovery is on average longer than hospital admission to death. While the full recovery is important for economy, hospitalisation length is more important for the state of healthcare system. The median hospitalisation length is 11 days (95% CI 10-13) for non-severe cases and 13 days for severe (95% CI 11-17) [26]. Both are log-normally distributed. For ensemble computations, their medians are further log-normally distributed according to their respective confidence intervals.

Similar numbers: mean (larger than median for lognormal distribution) hospital length of stay and ICU length of stay are 11 days (95% CI 7-14) and 8 days (95% CI 4-12) were reported by Zhou et al. [29].

Other parameters - review!? Fatality ratio of severe cases in need of intensive care is 50%. Fatality ratio of severe cases without intensive care is normally distributed with mean of 90% and $\sigma = 5\%$. Fatality ratio of severely ill without oxygen is 10% with $\sigma = 5\%$.

2.4 Initial condition

The initial condition for the simulation is defined for March 12, 2020. To that day, there were 131 symptomatic cases who tested positive, 8 days after first positive case, which implies an anomalously low doubling time of $\tau = 1.23$ days. This number is case specific as there was winter holiday in Slovenia at the end of February and beginning of Match, when lots of people went skiing to Italy (including Lombardy). Most of the initial cases were imported [??]. Other studies typically suggest a doubling time of around 5 days (95% CI 4.3 - 6.2) in the initial uncontrolled stage of the epidemic [30]. However, Abbott et al. [31] report smaller values of around 3.5 days in most of Western Europe. Thus, our choice is doubling time of $T_{double} = 3.5$ days, normally distributed with $\sigma = 0.5$.

Different numbers of actually infected people were suggested in the media reports, ranging from 5 to 10 times the number of reported positive cases. Given the average incubation period of 5 days + (1 day for visit) and somewhat smaller doubling period of 3.5 days, factor $2^{\frac{T_{inc}+1}{T_{double}}} = 3.3$ applies. Furthermore, the proportion of asymptomatic cases is around 18% based on the data from Diamond Princess Cruise Ship [32] (mostly older people) and around 33% based on the more recent study [33]. There have been reports from Iceland and an Italian town Vo which underwent vast testing, that nearly 50% of positively tested are asymptomatic. We opt for 40%, normally distributed with std. of 10%. This means that more than 700 people were infected in Slovenia on March 12. Factor 5.5 is somewhat smaller than the assumption of Kucharski et al. that only 16% of onsets are known `https://cmmid.github.io/topics/covid19/current-patterns-transmission/wuhan-early-dynamics.html`.

Based on the exponential growth in initial stage and incubation period, we randomly generate the infection length of the patients with exponential distribution with shape factor of 4.9, so that 131 people have infection for more than 5 days and develop symptoms. Initial distribution of 131 infected people by the time-length of their infection is shown in Figure 8. Note that in reality, due to many imported cases, the actual distribution may be different.

2.5 Limitations

- Nodes do not have age as property.
- Contacts are not distributed by age. Older have less connections.
- ...

3 Results

3.1 The effect of superspreaders

TBD

3.2 Prediction for Slovenia issued on March 28, 2020

Predictions of the evolution of COVID-19 pandemic are issued daily. New data is taken into account to correct the forecast. However, to accurately simulate the impact of government action

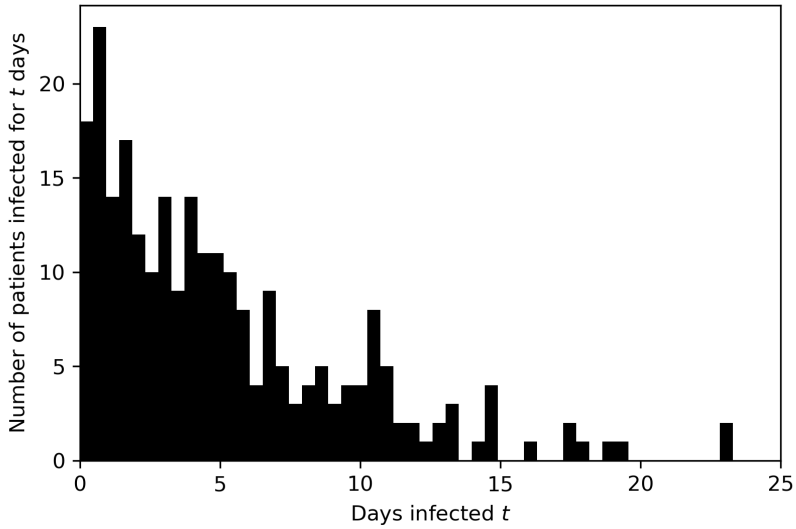

Figure 8: Distribution of 131 infected people on March 12, 2020, in Slovenia, by the time-length of their infection.

in advance, connectivity data of our real social network should be provided, e.g. based on the mobile phone traces etc.

Forecast issued on March 28, 2020, simulated from the initial condition on March 12, 2020 is avaiable at `https://fiz.fmf.uni-lj.si/~zaplotnikz/2020_03_28/` and is shown in Figure 9. 750 ensemble members were used to compute the uncertainty of the prediction. The likely outcome of the epidemics is within 25th and 75th percentile.

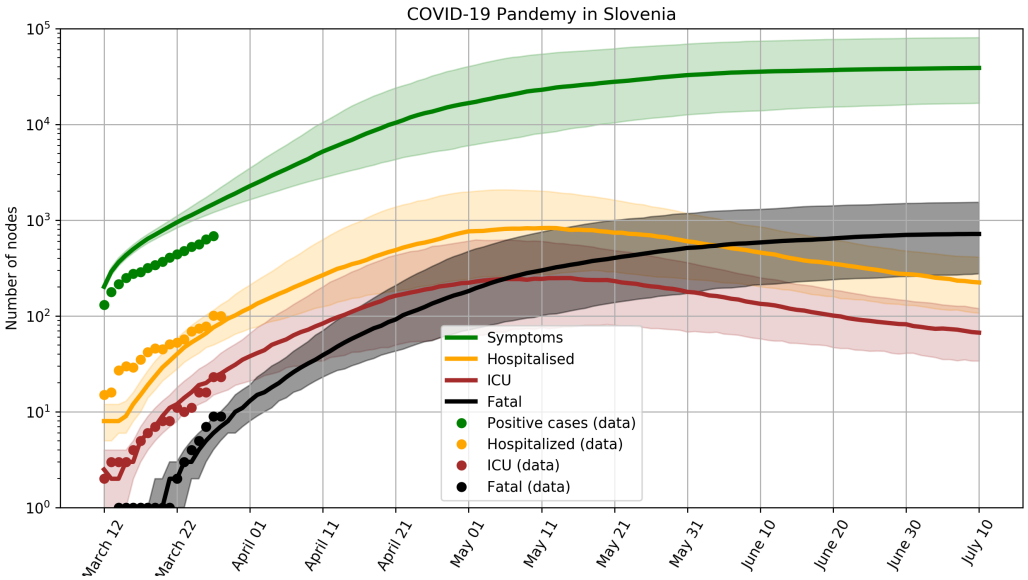

Figure 9: Forecast of COVID-19 pandemic in Slovenia issued on March 28, 2020 and comparison with real data. Median values along with 25th-75th percentiles of the ensemble members spread are shown.

Long-term forecast with present action is shown in Figure 10. Note that with the existing quarantine measures, the epidemics will not go away, we are just going to slow it down and to flatten the curve. Existing quarantine measures might not be efficient for such long time. Some options to control it faster are shown in the following section.

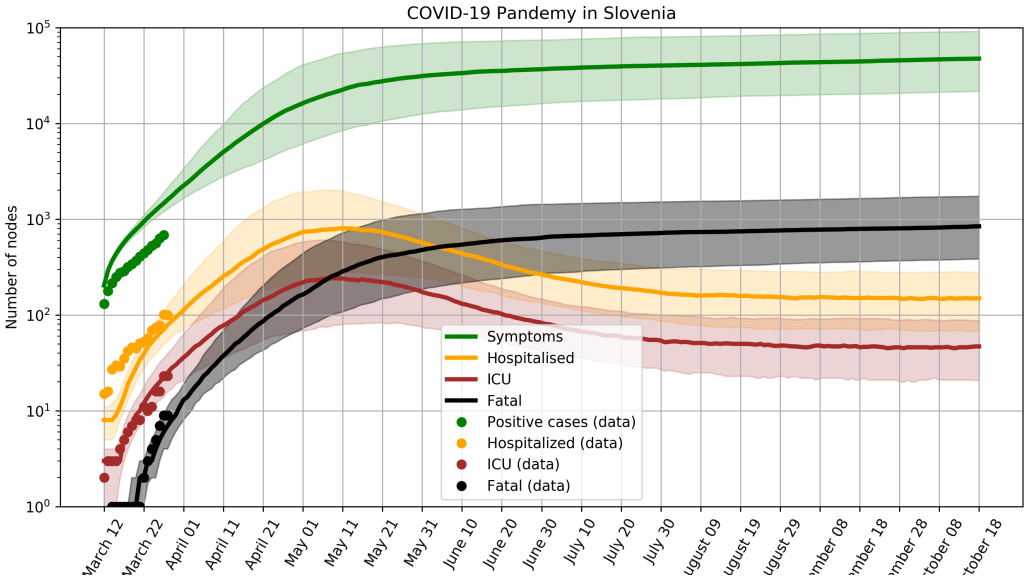

Figure 10: Same as Figure 9 but for 220 day interval.

4 Strategy

The main strategic points would be:

- Quarantine should be as strict as possible to prevent epidemics lasting too long.
- Restriction of travels, which prevents community-to-community spread [34].
- Introduce central quarantine unit for infected (strict isolation from their families) to prevent spread of the disease to household members, from which the transmission is most probable [3, 30]. Social distancing alone is not enough.
- Tracing of potential secondary and tertiary contacts and quarantine. Bi et al. [20] have shown that while the cases were isolated on average 4.6 days after developing symptoms, contact tracing reduced this by 1.9 days.
- Telecommunication data or mobile app data would be needed to track the potential secondary (or even tertiary) contacts.
- Use telecommunication data to analyse the connectivity of the social network. This way, we could could immediately simulate the effect of government action.
- Recent study (under review) has shown, that contact tracing is successful only for the case of low R_0 [35]. For example, around 50% (70%) of cases would need to be traced for $R_0 = 1.5(2.5)$ if we are to controll the outbreak.
- Widespread testing and inclusion of recovered back into society.

- The survival ability of SARS coronavirus in human specimens and their environments is relatively strong, however UV and heating (such as in cars exposed to sun, playgrounds etc.) dan efficiently eliminate the viral infectivity [36] and reduce the environmental transmission.

Further strategy to control the epidemics can be found at `https://www.endcoronavirus.org/`.

4.1 Central quarantine or isolation away from family members, nursing home residents and others

Strict isolation away from family members and other contacts is ordered from April 1 on. Epidemic evolution is shown in Figure 11. Note that at the peak of the pandemics at the end of April and the beginning of May, the number of patients requiring ICU drops by half from 220 to just around 110 with existing quarantine orders. The number of hospitalised patients would similarly fall from around 800 to 400.

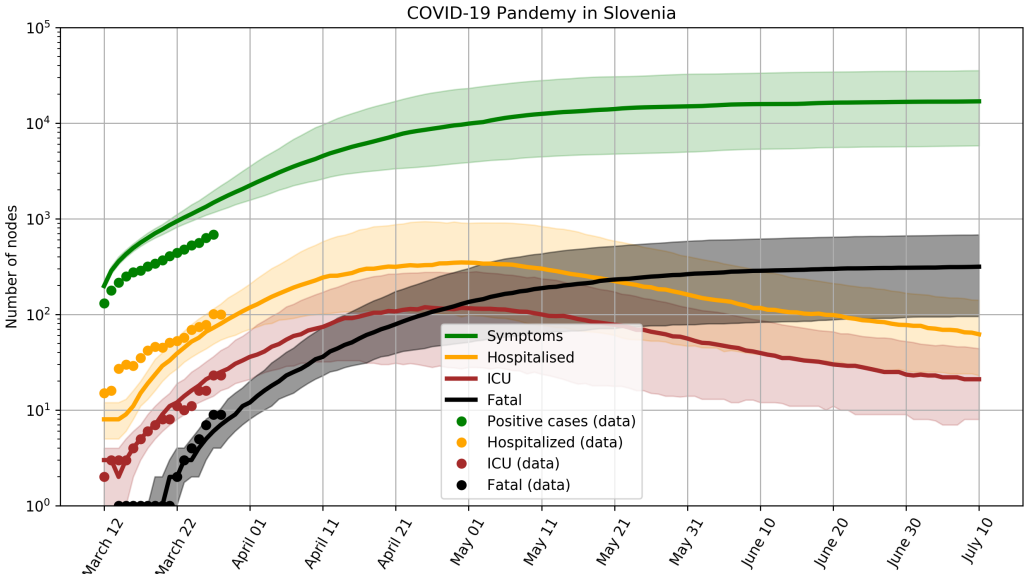

Figure 11: Same as Figure 9 but for strict isolation of symptomatic cases from April 1 on.

4.2 Quarantine of secondary infections

We can define illness onset (developed symptoms) to isolation function, similarly as inHellewell et al. [35]. Two parameters are important: percentage of tracked and the delay. Isolation efficiency is assumed 100%. In the case of short delay, we track and isolate potentially infected before they develop symptoms, but in the case of long delay, we only isolate them when they start developing symptoms.

TBD

TBD

5 Conclusions

Accurate models of the real-world social networks are needed to realistically simulate the topological dynamics of the epidemics. Similarly to Numerical Weather Prediction models [5, 37], the real connectivity data obtained by postprocessing of the phone traces, should be rapidly assimilated

into the virus spread prognostic model [e.g. 38]. This would allow 1) to estimate the critical virus spread parameters, needed for accurate forecasts of the pandemics, and 2) to better prepare a strategy of the virus containment, potentially saving thousands of lives, minimizing the economic damage and enhancing people's mobility.

Further work

Acknowledgments

The authors are grateful to Aleks Jakulin () Miha Kadunc (Sinergise) and Luka Renko (COVID-19 sledilnik) for providing the timely COVID-19 pandemics data for Slovenia. Žiga Zaplotnik would like to thank prof. Alojz Kodre and Simon Čopar for introducing him the node-based analysis of the information spread. Arthur Breitman is thanked for an interesting question on the basic properties of the virus transmission dynamics related to superspreaders. We thank fellow physicists Nejc Davidovič, Jan Bohinec and Luka Medic. Special thanks go to Roman Jerala and Tomaž Zwitter for discussions of the model, and for reading and commenting the scripts as well as providing useful literature.

References

[1] William Ogilvy Kermack and A. G. McKendrick. A contribution to the mathematical theory of epidemics. *Proceedings of the Royal Society of London. Series A, Containing Papers of a Mathematical and Physical Character*, 115(772):700–721, aug 1927. ISSN 0950-1207. doi: 10.1098/rspa.1927.0118.

[2] Herbert W Hethcote. The Mathematics of Infectious Diseases *. Technical Report 4, 2000. URL `http://www.siam.org/journals/sirev/42-4/37190.html`.

[3] Chaolong Wang, Li Liu, Xingjie Hao, Huan Guo, Qi Wang, Jiao Huang, Na He, Hongjie Yu, Xihong Lin, An Pan, Sheng Wei, and Tangchun Wu. Evolving Epidemiology and Impact of Non-pharmaceutical Interventions on the Outbreak of Coronavirus Disease 2019 in Wuhan, China. *medRxiv*, page 2020.03.03.20030593, mar 2020. doi: 10.1101/2020.03.03.20030593.

[4] Michael Y. Li, John R. Graef, Liancheng Wang, and János Karsai. Global dynamics of a SEIR model with varying total population size. *Mathematical Biosciences*, 160(2):191–213, aug 1999. ISSN 00255564. doi: 10.1016/S0025-5564(99)00030-9.

[5] Eugenia Kalnay. *Atmospheric modeling, data assimilation, and predictability*, volume 54. 2003. ISBN 9780521791793. doi: 10.1256/003590003606835 11.

[6] William A. Lahoz and Philipp Schneider. Data assimilation: making sense of Earth Observation. *Frontiers in Environmental Science*, 2(May):1–28, 2014. ISSN 2296-665X. doi: 10.3389/fenvs.2014.00016. URL `http://journal.frontiersin.org/article/10.3389/fenvs.2014.00016/abstract`.

[7] M. S. Bartlett. Measles Periodicity and Community Size. *Journal of the Royal Statistical Society. Series A (General)*, 120(1):48, 1957. ISSN 00359238.

[8] Li Qun Fang, Yang Yang, Jia Fu Jiang, Hong Wu Yao, David Kargbo, Xin Lou Li, Bao Gui Jiang, Brima Kargbo, Yi Gang Tong, Ya Wei Wang, Kun Liu, Abdul Kamara, Foday Dafae, Alex Kanu, Rui Ruo Jiang, Ye Sun, Ruo Xi Sun, Wan Jun Chen, Mai Juan Ma, Natalie E. Dean, Harold Thomas, Ira M. Longini, M. Elizabeth Halloran, and Wu Chun Cao. Transmission dynamics of Ebola virus disease and intervention effectiveness in Sierra Leone. *Proceedings of the National Academy of Sciences of the United States of America*, 113(16):4488–4493, apr 2016. ISSN 10916490. doi: 10.1073/pnas.1518587113.

[9] Qun Li, Xuhua Guan, Peng Wu, Xiaoye Wang, Lei Zhou, Yeqing Tong, Ruiqi Ren, Kathy S.M. Leung, Eric H.Y. Lau, Jessica Y. Wong, Xuesen Xing, Nijuan Xiang, Yang Wu, Chao Li, Qi Chen, Dan Li, Tian Liu, Jing Zhao, Man Liu, Wenxiao Tu, Chuding Chen, Lianmei Jin, Rui Yang, Qi Wang, Suhua Zhou, Rui Wang, Hui Liu, Yinbo Luo, Yuan Liu, Ge Shao, Huan Li, Zhongfa Tao, Yang Yang, Zhiqiang Deng, Boxi Liu, Zhitao Ma, Yanping Zhang, Guoqing Shi, Tommy T.Y. Lam, Joseph T. Wu, George F. Gao, Benjamin J. Cowling, Bo Yang, Gabriel M. Leung, and Zijian Feng. Early Transmission Dynamics in Wuhan, China, of Novel Coronavirus–Infected Pneumonia. *New England Journal of Medicine*, jan 2020. ISSN 0028-4793. doi: 10.1056/nejmoa2001316.

[10] Danilo Dolenc. Vsaka peta dvostarševska družina je zunajzakonska skupnost, 2018. URL `https://www.stat.si/StatWeb/News/Index/7725`.

[11] Lada A. Adamic, Rajan M. Lukose, Amit R. Puniyani, and Bernardo A. Huberman. Search in power-law networks. *Physical Review E - Statistical Physics, Plasmas, Fluids, and Related Interdisciplinary Topics*, 64(4):8, sep 2001. ISSN 1063651X. doi: 10.1103/PhysRevE.64.046135.

[12] Joseph Norman, Yaneer Bar-Yam, and Nicholas Taleb. Systemic Risk of Pandemic via Novel Pathogens-Coronavirus: A Note. Technical report, 2020.

[13] S. Y. Del Valle, J. M. Hyman, H. W. Hethcote, and S. G. Eubank. Mixing patterns between age groups in social networks. *Social Networks*, 29(4):539–554, oct 2007. ISSN 03788733. doi: 10.1016/j.socnet.2007.04.005.

[14] Joël Mossong, Niel Hens, Mark Jit, Philippe Beutels, Kari Auranen, Rafael Mikolajczyk, Marco Massari, Stefania Salmaso, Gianpaolo Scalia Tomba, Jacco Wallinga, Janneke Heijne, Malgorzata Sadkowska-Todys, Magdalena Rosinska, and W. John Edmunds. Social contacts and mixing patterns relevant to the spread of infectious diseases. *PLoS Medicine*, 5(3):0381–0391, mar 2008. ISSN 15491277. doi: 10.1371/journal.pmed.0050074.

[15] Joseph T. Wu, Kathy Leung, and Gabriel M. Leung. Nowcasting and forecasting the potential domestic and international spread of the 2019-nCoV outbreak originating in Wuhan, China: a modelling study. *The Lancet*, 395(10225):689–697, feb 2020. ISSN 1474547X. doi: 10.1016/S0140-6736(20)30260-9.

[16] Adam J Kucharski, Timothy W Russell, Charlie Diamond, Yang Liu, CMMID nCoV working Group, John Edmunds, Sebastian Funk, and Rosalind M Eggo. Early dynamics of transmission and control of COVID-19: a mathematical modelling study. *medRxiv*, page 2020.01.31.20019901, feb 2020. doi: 10.1101/2020.01.31.20019901.

[17] Ying Liu, Albert A Gayle, Annelies Wilder-Smith, and Joacim Rocklöv. The reproductive number of COVID-19 is higher compared to SARS coronavirus. *Journal of Travel Medicine*, 2020:1–4, 2020. doi: 10.1093/jtm/taaa021. URL `https://academic.oup.com/jtm/article-abstract/27/2/taaa021/5735319`.

[18] Yang Liu, Rosalind M Eggo, and Adam J Kucharski. Secondary attack rate and superspreading events for SARS-CoV-2. *The Lancet*, 395(10227):e47, mar 2020. ISSN 0140-6736. doi: 10.1016/S0140-6736(20)30462-1.

[19] Rachel M. Burke, Claire M. Midgley, Alissa Dratch, Marty Fenstersheib, Thomas Haupt, Michelle Holshue, Isaac Ghinai, M. Claire Jarashow, Jennifer Lo, Tristan D. McPherson, Sara Rudman, Sarah Scott, Aron J. Hall, Alicia M. Fry, and Melissa A. Rolfes. Active Monitoring of Persons Exposed to Patients with Confirmed COVID-19 — United States, January–February 2020. *MMWR. Morbidity and Mortality Weekly Report*, 69(9):245–246, mar 2020. ISSN 0149-2195. doi: 10.15585/mmwr.mm6909e1. URL `http://www.cdc.gov/mmwr/volumes/69/wr/mm6909e1.htm?s{_}cid=mm6909e1{_}w`.

[20] Qifang Bi, Yongsheng Wu, Shujiang Mei, Chenfei Ye, Xuan Zou, Zhen Zhang, Xiaojian Liu, Lan Wei, Shaun A Truelove, Tong Zhang, Wei Gao, Cong Cheng, Xiujuan Tang, Xiaoliang Wu, Yu Wu, Binbin Sun, Suli Huang, Yu Sun, Juncen Zhang, Ting Ma, Justin Lessler, and Teijian Feng. Epidemiology and Transmission of COVID-19 in Shenzhen China: Analysis of 391 cases and 1,286 of their close contacts. *medRxiv*, page 2020.03.03.20028423, mar 2020. doi: 10.1101/2020.03.03.20028423.

[21] Robert Verity, Lucy C Okell, Ilaria Dorigatti, Peter Winskill, Charles Whittaker, Natsuko Imai, Gina Cuomo-Dannenburg, Hayley Thompson, Patrick Walker, Han Fu, Amy Dighe, Jamie Griffin, Anne Cori, Marc Baguelin, Sangeeta Bhatia, Adhiratha Boonyasiri, Zulma M Cucunuba, Rich Fitzjohn, Katy A M Gaythorpe, Will Green, Arran Hamlet, Wes Hinsley, Daniel Laydon, Gemma Nedjati-Gilani, Steven Riley, Sabine Van-Elsand, Erik Volz, Haowei Wang, Yuanrong Wang, Xiayoue Xi, Christl Donnelly, Azra Ghani, and Neil Ferguson. Estimates of the severity of COVID-19 disease. *medRxiv*, page 2020.03.09.20033357, mar 2020. doi: 10.1101/2020.03.09.20033357.

[22] Timothy W. Russell, Joel Hellewell, Sam Abbott, Christopher I Jarvis, Kevin van Zandvoort, Ruwan Ratnayake, Working Group CMMID NCov, Stefan Flasche, Rosalind Eggo, John Edmunds, and Adam J Kucharski. Using a delay-adjusted case fatality ratio to estimate under-reporting — CMMID Repository, 2020. URL `https://cmmid.github.io/topics/covid19/severity/global{_}cfr{_}estimates.html`.

[23] Joseph T. Wu, Kathy Leung, Mary Bushman, Nishant Kishore, Rene Niehus, Pablo M. de Salazar, Benjamin J. Cowling, Marc Lipsitch, and Gabriel M. Leung. Estimating clinical severity of COVID-19 from the transmission dynamics in Wuhan, China. *Nature Medicine*, pages 1–5, mar 2020. ISSN 1078-8956. doi: 10.1038/s41591-020-0822-7. URL `http://www.nature.com/articles/s41591-020-0822-7`.

[24] Neil M Ferguson, Daniel Laydon, Gemma Nedjati-Gilani, Natsuko Imai, Kylie Ainslie, Marc Baguelin, Sangeeta Bhatia, Adhiratha Boonyasiri, Zulma Cucunubá, Gina Cuomo-Dannenburg, Amy Dighe, Ilaria Dorigatti, Han Fu, Katy Gaythorpe, Will Green, Arran Hamlet, Wes Hinsley, Lucy C Okell, Sabine Van Elsland, Hayley Thompson, Robert Verity, Erik Volz, Haowei Wang, Yuanrong Wang, Patrick Gt Walker, Caroline Walters, Peter Winskill, Charles Whittaker, Christl A Donnelly, Steven Riley, and Azra C Ghani. Impact of non-pharmaceutical interventions (NPIs) to reduce COVID-19 mortality and healthcare demand. *COVID-19 Reports*, 9, 2020. doi: 10.25561/77482. URL `https://doi.org/10.25561/77482`.

[25] PopulationPyramid.net. Population Pyramid. URL `https://www.populationpyramid.net/slovenia/2019/`.

[26] Natalie M Linton, Tetsuro Kobayashi, Yichi Yang, Katsuma Hayashi, Andrei R Akhmetzhanov, Sung-Mok Jung, Baoyin Yuan, Ryo Kinoshita, and Hiroshi Nishiura. Incubation Period and Other Epidemiological Characteristics of 2019 Novel Coronavirus Infections with Right Truncation: A Statistical Analysis of Publicly Available Case Data. *Journal of clinical medicine*, 9(2), feb 2020. ISSN 2077-0383. doi: 10.3390/jcm9020538. URL `http://www.ncbi.nlm.nih.gov/pubmed/32079150`.

[27] Tao Liu, Jianxiong Hu, Min Kang, Lifeng Lin, Haojie Zhong, Jianpeng Xiao, Guanhao He, Tie Song, Qiong Huang, Zuhua Rong, Aiping Deng, Weilin Zeng, Xiaohua Tan, Siqing Zeng, Zhihua Zhu, Jiansen Li, Donghua Wan, Jing Lu, Huihong Deng, Jianfeng He, and Wenjun Ma. Time-varying transmission dynamics of Novel Coronavirus Pneumonia in China. *bioRxiv*, page 2020.01.25.919787, jan 2020. doi: 10.1101/2020.01.25.919787. URL `https://www.biorxiv.org/content/10.1101/2020.01.25.919787v1`.

[28] Roman Woelfel, Victor Max Corman, Wolfgang Guggemos, Michael Seilmaier, Sabine Zange, Marcel A Mueller, Daniela Niemeyer, Patrick Vollmar, Camilla Rothe, Michael Hoelscher, Tobias Bleicker, Sebastian Bruenink, Julia Schneider, Rosina Ehmann, Katrin Zwirglmaier,

Christian Drosten, and Clemens Wendtner. Clinical presentation and virological assessment of hospitalized cases of coronavirus disease 2019 in a travel-associated transmission cluster. *medRxiv*, page 2020.03.05.20030502, mar 2020. doi: 10.1101/2020.03.05.20030502.

[29] Fei Zhou, Ting Yu, Ronghui Du, Guohui Fan, Ying Liu, Zhibo Liu, Jie Xiang, Yeming Wang, Bin Song, Xiaoying Gu, Lulu Guan, Yuan Wei, Hui Li, Xudong Wu, Jiuyang Xu, Shengjin Tu, Yi Zhang, Hua Chen, and Bin Cao. Clinical course and risk factors for mortality of adult inpatients with COVID-19 in Wuhan, China: a retrospective cohort study. *The Lancet*, 0(0), mar 2020. ISSN 01406736. doi: 10.1016/s0140-6736(20)30566-3.

[30] Luca Ferretti, Chris Wymant, Michelle Kendall, Lele Zhao, Anel Nurtay, David G Bonsall, and Christophe Fraser. Quantifying dynamics of SARS-CoV-2 transmission suggests that epidemic control and avoidance is feasible through instantaneous digital contact tracing. *medRxiv*, page 2020.03.08.20032946, mar 2020. doi: 10.1101/2020.03.08.20032946. URL `https://www.medrxiv.org/content/10.1101/2020.03.08.20032946v1`.

[31] Sam Abbott, Joel Hellewell, James D Munday, June Young Chun, Robin N. Thompson, Nikos I Bosse, Yung-Wai Desmond Chan, Timothy W Russell, Christopher Jarvis, Stefan Flasche, Adam J Kucharski, Rosalind Eggo, and Sebastian Funk. Temporal variation in transmission during the COVID-19 outbreak — CMMID Repository, 2020. URL `https://cmmid.github.io/topics/covid19/current-patterns-transmission/global-time-varying-transmission.html`.

[32] Kenji Mizumoto, Katsushi Kagaya, Alexander Zarebski, and Gerardo Chowell. Estimating the asymptomatic proportion of coronavirus disease 2019 (COVID-19) cases on board the Diamond Princess cruise ship, Yokohama, Japan, 2020. *Eurosurveillance*, 25(10):2000180, mar 2020. ISSN 1560-7917. doi: 10.2807/1560-7917.es.2020.25.10.2000180.

[33] Hiroshi Nishiura, Tetsuro Kobayashi, Takeshi Miyama, Ayako Suzuki, Sungmok Jung, Katsuma Hayashi, Ryo Kinoshita, Yichi Yang, Baoyin Yuan, Andrei R Akhmetzhanov, and Natalie M Linton. Estimation of the asymptomatic ratio of novel coronavirus (2019-nCoV) infections among passengers on evacuation flights, feb 2020.

[34] Alexander F Siegenfeld and Yaneer Bar-Yam. Working Paper Eliminating COVID-19: A Community-based Analysis. Technical report, 2020.

[35] Joel Hellewell, Sam Abbott, Amy Gimma, Nikos I Bosse, Christopher I Jarvis, Timothy W Russell, James D Munday, Adam J Kucharski, W John Edmunds, CMMID nCoV working Group, Sebastian Funk, and Rosalind M Eggo. Feasibility of controlling 2019-nCoV outbreaks by isolation of cases and contacts. *medRxiv*, page 2020.02.08.20021162, feb 2020. doi: 10.1101/2020.02.08.20021162.

[36] Shu Ming Duan, Xin Sheng Zhao, Rui Fu Wen, Jing Jing Huang, Guo Hua Pi, Su Xiang Zhang, Jun Han, Sheng Li Bi, L. Ruan, and Xiao Ping Dong. Stability of SARS Coronavirus in Human Specimens and Environment and Its Sensitivity to Heating and UV Irradiation. *Biomedical and Environmental Sciences*, 16(3):246–255, sep 2003. ISSN 08953988.

[37] Peter Bauer, Alan Thorpe, and Gilbert Brunet. The quiet revolution of numerical weather prediction, sep 2015. ISSN 14764687.

[38] Zhidong Cao, Qingpeng Zhang, Xin Lu, Dirk Pfeiffer, Lei Wang, Hongbing Song, Tao Pei, Zhongwei Jia, and Daniel Dajun Zeng. Incorporating Human Movement Data to Improve Epidemiological Estimates for 2019-nCoV. *medRxiv*, page 2020.02.07.20021071, feb 2020. doi: 10.1101/2020.02.07.20021071. URL `http://medrxiv.org/content/early/2020/02/09/2020.02.07.20021071.abstract`.

[39] Pearu Peterson. F2PY: a tool for connecting Fortran and Python programs. *International Journal of Computational Science and Engineering*, 4(4):296–305, 2009.

Code availability

The model is freely available at `https://github.com/zaplotnik/korona/code`. The core program is written in Python 2.7 and requires standard `scipy`, `numpy` and `matplotlib` libraries. Computationally critical parts of the program are written in Fortran. Python bindings are created using F2PY [39]

```
f2py -c generate_connections.f90 -m generate_connections
```

Fortran random number generator (`random.f90`) is taken from Allan Miller's Fortran Software repository `https://jblevins.org/mirror/amiller/`.